Molecular Cell, Vol. 6, 885–897, October, 2000, Copyright ©2000 by Cell Press

Crystal Structure of a Flp Recombinase–Holliday Junction Complex: Assembly of an Active Oligomer by Helix Swapping

Yu Chen,* Umadevi Narendra,*§ Lisa E. Iype,†‖ Michael M. Cox,† and Phoebe A. Rice*‡
*Department of Biochemistry and Molecular Biology
University of Chicago
Chicago, Illinois 60637
†Department of Biochemistry
University of Wisconsin
Madison, Wisconsin 53706

Summary

The crystal structure of a Flp recombinase tetramer bound to a Holliday junction intermediate has been determined at 2.65 Å resolution. Only one of Flp's two domains, containing the active site, is structurally related to other λ integrase family site-specific recombinases, such as Cre. The Flp active site differs, however, in that the helix containing the nucleophilic tyrosine is domain swapped, such that it cuts its DNA target in *trans.* The Flp tetramer displays pseudo four-fold symmetry matching that of the square planar Holliday junction substrate. This tetramer is stabilized by additional novel *trans* interactions among monomers. The structure illustrates how mechanistic unity is maintained on a chemical level while allowing for substantial variation on the structural level within a family of enzymes.

Introduction

Flp, encoded by the 2 μm plasmid of the yeast *Saccharomyces cerevisiae*, is a member of the λ integrase or tyrosine-based family of site-specific DNA recombinases. These enzymes use the same basic chemistry under different circumstances to accomplish a variety of tasks, including inserting bacteriophage DNA into host genomes, altering patterns of gene expression, mobilizing certain mobile genetic elements, and promoting proper segregation of replicons (reviewed in Esposito and Scocca, 1997; Nunes-Duby et al., 1998). Flp-mediated recombination allows amplification of the 2 μm plasmid copy number during replication (reviewed in Sadowski, 1995).

Several of these systems have been extensively characterized in vitro. Flp and Cre are the simplest of these, requiring no accessory proteins or DNA sequences, and both have been employed in an ever-widening range of applications in cell and molecular biology. Both enzymes function in vivo in a variety of organisms and will promote inversions, deletions, and insertions of DNA segments, depending only upon the arrangement of recombination sites (O'Gorman and Wahl, 1997; Nagy, 2000).

Flp is one of only a few known eukaryotic members of the λ integrase family. It is highly diverged in sequence from the prokaryotic members (its catalytic domain is only 13% identical to Cre's), and as discussed below, its active site is assembled differently. It has therefore been unclear to what degree the mechanistic similarities described below would be supported by structural similarities.

Crystal structures of four members of this family have been determined: the core domains of the λ (Kwon et al., 1997) and HP1 (Hickman et al., 1997) phage integrases, intact E. coli XerD (Subramanya et al., 1997), and the entire DNA complex of phage P1 Cre (Guo et al., 1997). These proteins share a structurally conserved active site–containing domain that is also found in the eukaryotic type IB topoisomerases, reflecting a mechanistic relationship (Cheng et al., 1998; Redinbo et al., 1998). The helical portion of this fold resembles two helix-turn-helix motifs and is also found in the AraC family of transcriptional regulators (Gillette et al., 2000).

Cre has been crystallized with a variety of DNA substrates, defining different steps along the reaction pathway (Guo et al., 1997, 1999; Gopaul et al., 1998). The complex is always a tetramer with pseudo-four-fold symmetry matching that of the square planar Holliday junction that is the reaction intermediate. This work showed that the entire Cre-mediated recombination reaction requires only relatively minor conformational changes in the synaptic complex.

The reaction pathway proposed for this family of recombinases is shown in Figure 1. The DNA recombination sites vary in complexity, but they always include two binding sites for the recombinase that are inverted about a 6–8 bp spacer. Two recombination sites are brought together, and one strand from each is cleaved by direct attack of an active site tyrosine, creating a transient covalent 3′-phosphotyrosyl linkage. The free 5′ ends are exchanged, and the 5′ hydroxyls attack the opposite phosphotyrosyl linkage, forming a Holliday junction intermediate. A second and similar set of cleavage and strand exchange steps completes the recombination reaction. This stepwise strand exchange mechanism requires half-of-the-sites activity in the recombinase tetramer, and a central isomerization step that determines which pair of catalytic centers is active. This pathway is supported by the Cre–DNA structures and biochemical studies of several family members (Hallet et al., 1999, reviewed in Gopaul and Van Duyne, 1999). Type IB topoisomerases also form a 3′-phosphotyrosyl intermediate but function as monomers and religate the original DNA strand after allowing torsional relaxation.

In addition to the nucleophilic tyrosine, the active sites of these recombinases and the type IB topoisomerases contain several other highly conserved residues (Argos et al., 1986; Abremski and Hoess, 1992; reviewed in Grainge and Jayaram, 1999). Three of these, R191, H305, and R308 in Flp, have been demonstrated to be catalytically important in Flp and several other systems, al-

‡To whom correspondence should be addressed (e-mail: price@midway.uchicago.edu).
§Present address: Department of Biochemistry, Case Western Reserve University, Cleveland, Ohio 44106.
‖Present address: Research Collaboratory for Structural Bioinformatics, and Rutgers, The State University of New Jersey, Piscataway, New Jersey 08854.

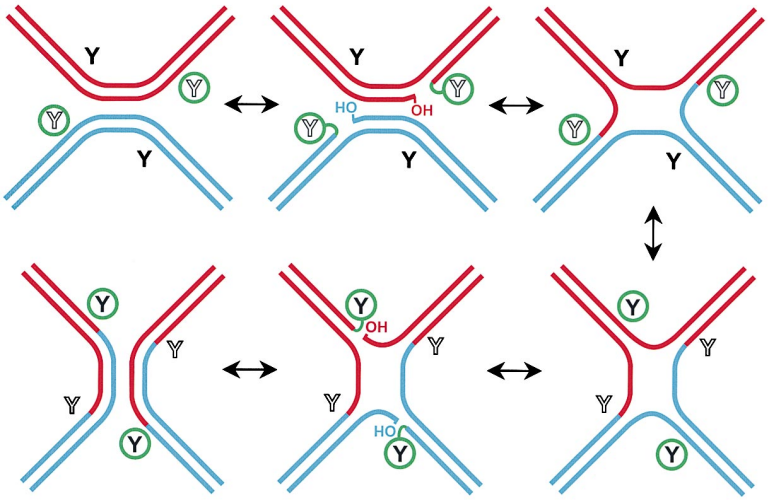

Figure 1. Proposed Mechanism of Site-Specific Recombination Catalyzed by the Tyrosine Recombinases

Two DNA segments are synapsed by a tetramer of the recombinase, carrying a tyrosine nucleophile in each active site. Only two of the four monomers are active at a given time, as indicated by the green circles. These tyrosines directly attack the scissile phosphodiester bonds, resulting in covalent 3′ phosphotyrosine intermediates. The 5′ hydroxyl subsequently attacks the opposite phosphotyrosine, leading to the formation of a Holliday junction intermediate. Isomerization of the complex activates the other pair of tyrosines, initiating a second round of DNA cleavage and strand exchange reactions, which resolves the Holliday junction into recombinant products.

though H305 is more important for religation than cleavage, and the equivalent lysine is not essential in the topoisomerases. These residues presumably localize the scissile phosphate and stabilize the transition state. The second arginine also binds a water molecule in human topo I that may be the general base that accepts a proton from the attacking tyrosine (Redinbo et al., 2000). Structural studies have highlighted two additional conserved residues: a lysine, and a tryptophan that is often replaced by histidine. This lysine in vaccinia virus topoisomerase has been shown to be the general acid that protonates the leaving 5′ hydroxyl (Krogh and Shuman, 2000). Sequence comparisons had tentatively identified these residues as K223 and W330 in Flp, which our structure confirms (Nunes-Duby et al., 1998).

In contrast to other integrase class recombinases, including the λ and HP1 phage integrases (Nunes-Duby et al., 1994; Hickman et al., 1997), Cre (Guo et al., 1997), and XerC and XerD (Arciszewska and Sherratt, 1995; Blakely et al., 1997), the active sites within Flp complexes are composed of amino acid residues from two different monomers (Chen et al., 1992; Lee et al., 1999, and references therein). Jayaram and colleagues showed that the active site tyrosine (Y343) is donated not by the monomer bound adjacent to the cleaved phosphodiester (called cleavage in *cis*), but by a monomer bound to one of the other three binding sites within the complex (cleavage in *trans*). This arrangement appears to be unique to Flp and closely related recombinases from other yeast plasmids (Yang and Jayaram, 1994). These results have led to much experimentation and speculation focused on the question of mechanistic unity within the λ integrase family of enzymes (Nunes-Duby et al., 1994; Jayaram, 1997; Huffman and Levene, 1999; Lee et al., 1999). Several lines of evidence (Qian and Cox, 1995; Voziyanov et al., 1999), but most notably the Cre structures, suggested a *trans* cyclic arrangement of Flp monomers in the complex. Although the active site of Cre is assembled in *cis,* the final helix of each monomer is nestled into a pocket on the adjacent monomer, forming a cyclic tetramer. This arrangement led to a proposal that the Flp recombinase could cleave in *trans* with the subunits in a similarly cyclic arrangement (Guo et al., 1997).

Another feature in which Flp differs from Cre is the length of the DNA spacer between cleavage sites. The Cre recombination site, loxP, has a 6 bp spacer, and recombination is very inefficient at sites with a 7 bp spacer (Sternberg and Hamilton, 1981; Hoess et al., 1982). Flp's natural recombination target (FRT) has an 8 bp spacer (Figure 2a), but it readily recombines artificial sites with 7 or 9 bp spacers (Senecoff and Cox, 1986). Changing the length of the DNA in the center of the complex would presumably change the relative orientations of the four monomers, raising the question of how the half-of-the-sites activity is maintained in such a flexible system.

To address these questions, we have determined the crystal structure of a Flp tetramer bound to a trapped Holliday junction intermediate. Only the core catalytic domain is structurally conserved between Flp and the related proteins discussed above. Even within this domain, the active site is indeed assembled differently—the helix containing the nucleophilic tyrosine is domain swapped. A second, unexpected *trans* interaction stabilizes the tetramer, and the loops flanking this second *trans* segment impart significant flexibility on the Flp synaptic complex. Although Cre and Flp exhibit very similar half-of-the-sites activity, the protein–protein contacts that presumably mediate communication among monomers differ. Despite these differences, the overall geometry of the Holliday junction in both complexes is similar. As Flp and Cre are so far diverged from one another that they may have evolved separately from ancestral topoisomerases, this geometry may be intrinsically favorable for recombination.

Results and Discussion

Characterization of the DNA in the Crystal

Flp protein was cocrystallized with a symmetrized FRT site that was designed as a suicide inhibitor (Figure 2b) (Nunes-Duby et al., 1987). A nick is placed one base away from the Flp cleavage site. Formation of the phosphotyrosine intermediate thus releases nucleotide # −4 into the bulk solution, carrying with it the hydroxyl that is needed as the nucleophile in the next step. This was

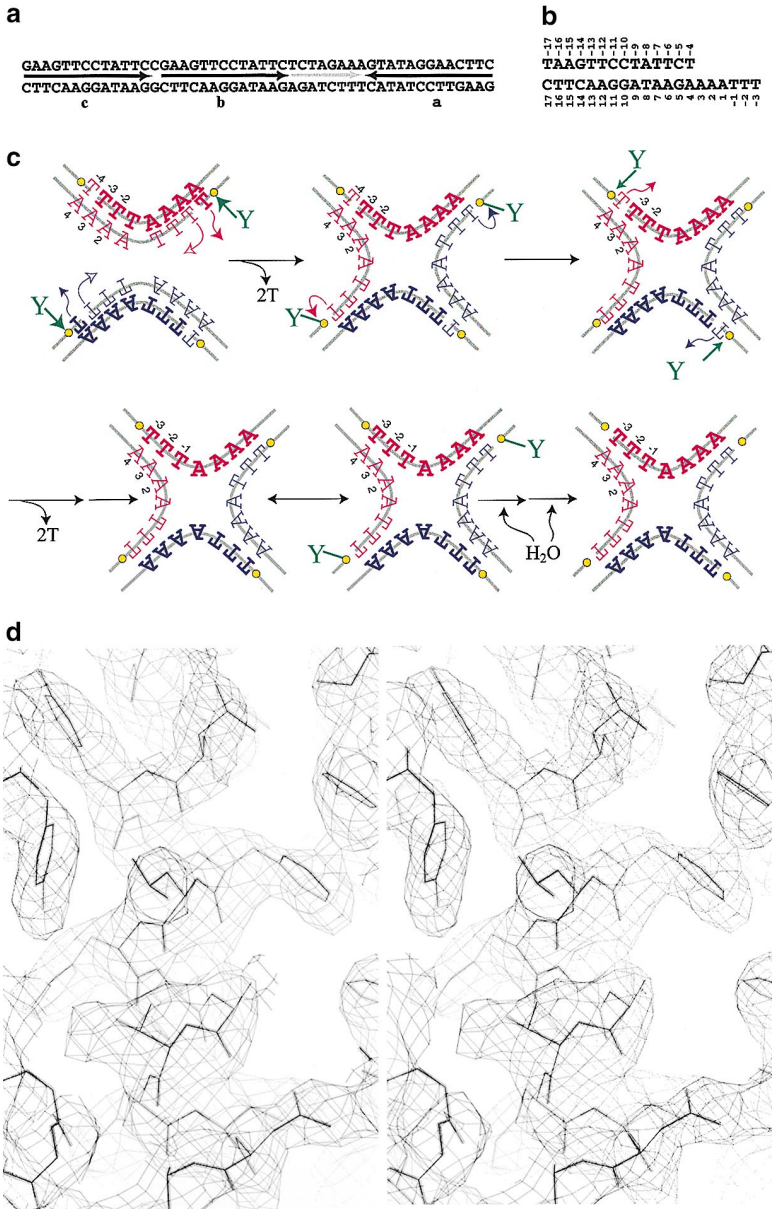

Figure 2. Crystallization and Structure Determination

(a) The natural Flp recombination target (FRT) site. It contains three Flp-binding sites (black arrows), but subsite c is unnecessary for recombination in vivo and in vitro. Flp cleaves at the 5′ ends of the 8 bp spacer (gray arrow). This spacer can vary in sequence, but recombination only occurs between sites with matching spacers.

(b) Symmetrized half-FRT site used in crystallization, numbered from center. Essentially identical crystals could be grown with a site lacking C17. This substrate provided the best crystals of at least eight that were screened in crystallization trials, three having the A/T spacer sequence shown.

(c) Pathway for formation of the Holliday junction present in the crystals. Four of the half-sites shown in (b) anneal to form two duplexes (red and blue) with nicks at the junction of bold and plain text. Only the sequence at the center is shown, and yellow circles represent the scissile phosphates. Due to the nicks, T −4 is lost into solution upon attack of the tyrosine. As the spacer sequence used allows slippage of the base pairing, T −3 of the opposite duplex can fit into the pocket vacated by T −4, and its 5′ hydroxyl can attack the phosphotyrosine intermediate. After isomerization, the same sequence of events can occur at the other pair of active sites, resulting in a Holliday junction with a central unpaired A. All four scissile bonds were hydrolyzed at some point before data collection. This probably occurred because the Holliday junction was in equilibrium with the phosphotyrosine intermediate, which is subject to slow hydrolysis.

(d) Stereo view of the experimental electron density map, after four-fold averaging, solvent flattening, and histogram matching. Helix G and adjacent residues are shown.

intended to trap the covalent protein–DNA intermediate (at the second step in Figure 1). However, the reaction proceeded to form a nicked Holliday junction intermediate with a 7 base spacer, as shown in Figure 2c. This was possible because (1) the sequence of our spacer allows the formation of 3 Watson-Crick base pairs adjacent to the active site in the "slipped" configuration shown, and (2) Flp efficiently recombines substrates whose spacer is one base shorter (or longer) than the WT FRT site (Senecoff and Cox, 1986). That T −4 had been replaced by T −3 on all four monomers was clear in experimental electron density maps calculated using data from crystals in which every T in the top strand (as shown in Figure 2b) had been replaced by 5-bromouracil. There was clear density for a pyrimidine in this position, but the anomalous difference Fourier showed no features on this base, compared to strong peaks for Br atoms on other, similarly well-ordered bases. There was also clear density for a phosphate on the 3′ side of this base, which was not expected for T −4, as the synthetic oligonucleotides used lacked terminal phosphates.

The phosphotyrosine intermediate is subject to slow hydrolysis and glycerolysis (Knudsen et al., 1997), and during refinement it became clear our complex had undergone such cleavage at some point before data collection. In all four monomers, the model that best fit the density contained nicked DNA and a free tyrosine, although a small fraction of monomers 1 and 2 may still be in the phosphotyrosine form. This cleavage was confirmed by denaturing gel electrophoresis of a redissolved crystal.

Structure Determination

The asymmetric unit of the crystals contains a tetramer of Flp protein bound to the Holliday junction substrate

Table 1. Data and Refinement Statistics

Data Collection and Phasing Statistics

	No. of Sites Major (Minor)	λ (Å)	Source	Resolution (Å)	Completeness (%)	R_{merge}[a] (%)	Phasing Power[b]
Native1		0.9795	14BM-D[c]	2.65	95.3	4.7	
Native2		0.9960	14BM-D	2.8	75.0	5.4	
Bromine1[d]	23	0.9202	14BM-D	3.1	95.4	8.9	
Bromine2	23	0.9196	14BM-D	3.1	92.5	10.0	0.53
Bromine3	23	0.8985	14BM-D	3.1	94.9	9.7	
Bromine4[d]	12	0.9201	14BM-D	3.1	92.7	9.8	0.54
Mercury1	5(9)	1.5418	Laboratory	3.2	97.8	10.5	1.72
Mercury2	5(6)	1.5418	Laboratory	3.0	97.2	11.6	1.46
Mercury3	1(5)	0.9960	14BM-D	2.9	98.0	9.8	0.92

Mean Figure of Merit (FOM)[e] for Phasing

Resolution (Å)	10.14	7.65	6.15	5.14	4.41	3.87	3.44	3.10	Total
FOM	0.7364	0.7365	0.7461	0.6957	0.6109	0.5031	0.4391	0.3758	0.5196

Final Native Data Set[f] and Refinement Statistics

Resolution (Å)	Completeness (% with F > 0)	R[g] (%)	R_{free}[g] (%)	Rms Deviations	
				Bond (Å)	Angle (°)
2.65	88.5	24.9	29.7	0.007	1.2

[a] $R_{merge} = \Sigma|I - \langle I\rangle|/\Sigma I$, in which $\langle I\rangle$ is the average intensity of a reflection.
[b] Phasing power $= \Sigma|F_H|/\Sigma||F_{PH\ obs}| - |F_{PH\ calc}||$.
[c] 14BM-D, Advanced Photon Source BioCARS14BM-D beamline, Argonne National Laboratory.
[d] Bromine1–3 were measured from the same bromine derivative using oligonucleotide T_{br4}, and Bromine4 from T_{br3}.
[e] FOM $= \langle\cos(\Delta\alpha)\rangle$, in which $\Delta\alpha$ means the estimated error in phase angle of a reflection.
[f] The initial native data set was obtained by merging native1 and native2; native2 provided the low-resolution data that were missing in native1. This data set was used in most of the refinement process, whereas native1 only was used in the final stages of refinement. The cutoff used in data processing, $I/\sigma I$, was -3, whereas the cutoff for refinement, $F/\sigma F$, was 0.
[g] $R = \Sigma|F_{obs} - F_{calc}|/\Sigma F_{obs}$; 10% of data were excluded from refinement and used as a test data set to calculate R_{free}.

described above (total molecular weight, 238 kDa). The structure was determined by a combination of multi-wavelength anomalous dispersion (MAD) and multiple isomorphous replacement with anomalous scattering (MIRAS) (see Experimental Procedures; Table 1). Initial phases were improved by solvent flattening, histogram matching, and averaging about the noncrystallographic symmetry (Figure 2d).

The final model is missing only a few turns that were too poorly ordered in the electron density map to be modeled. It has been refined to a resolution of 2.65 Å, resulting in working and free R factors of 24.9% and 29.7%, respectively. 85.6% of the nonglycine protein residues lie in the most preferred regions of the Ramachandran plot, as defined by PROCHECK (Laskowski et al., 1993).

The contacts among tetramers in the crystal are unusual in that the DNA ends do not stack together to form pseudo-continuous helices, but are either solvent exposed or packed onto the surfaces of neighboring complexes.

Overall Structure of the Complex

The DNA Holliday junction is held in a roughly square planar conformation by a tetramer of Flp protein (Figure 3). The complex has nearly perfect two-fold symmetry, but only approximate four-fold symmetry. Thus, each monomer is nearly identical to the one opposite it but differs from the two that flank it. As each of the four monomers is in a different crystal-packing environment, this symmetry cannot be an artifact of crystal-packing forces. The complex as a whole is a rather loosely packed, flexible entity. This reflects flexibility within individual monomers rather than a lack of intermolecular contacts.

The differences between the pairs of dyad-related monomers reflect the half-of-the-sites activity of the enzyme. As discussed in more detail below, monomers 1 and 2 (as numbered in Figure 3) appear to be in an active conformation, whereas the catalytic sites of monomers 3 and 4 are crippled by displacement of the nucleophilic tyrosine (Y343) away from the scissile phosphate. The relationship between the N- and C-terminal domains also differs by a few degrees between the two pairs of monomers. Monomers 3 and 4 are less well ordered than the other pair, particularly in their N-terminal domains. This correlates with the fact that they are less involved in crystal packing, but it could also reflect functional differences between the two pairs of monomers.

Based on a topological analysis of reaction products, the synaptic complexes of Flp and related recombinases were proposed to have a preferred chirality (Crisona et al., 1999). Although the out-of-plane bending of the two active arms of our Holliday junction (Figure 3b) is small, its handedness matches that predicted.

Structure of a Single Protomer

The Flp monomer is composed of two compact domains and two protruding segments that pack in *trans* onto neighboring protomers within the tetramer (Figure 3). The first such segment contains helix D and connects the two domains, and the second contains helix M and

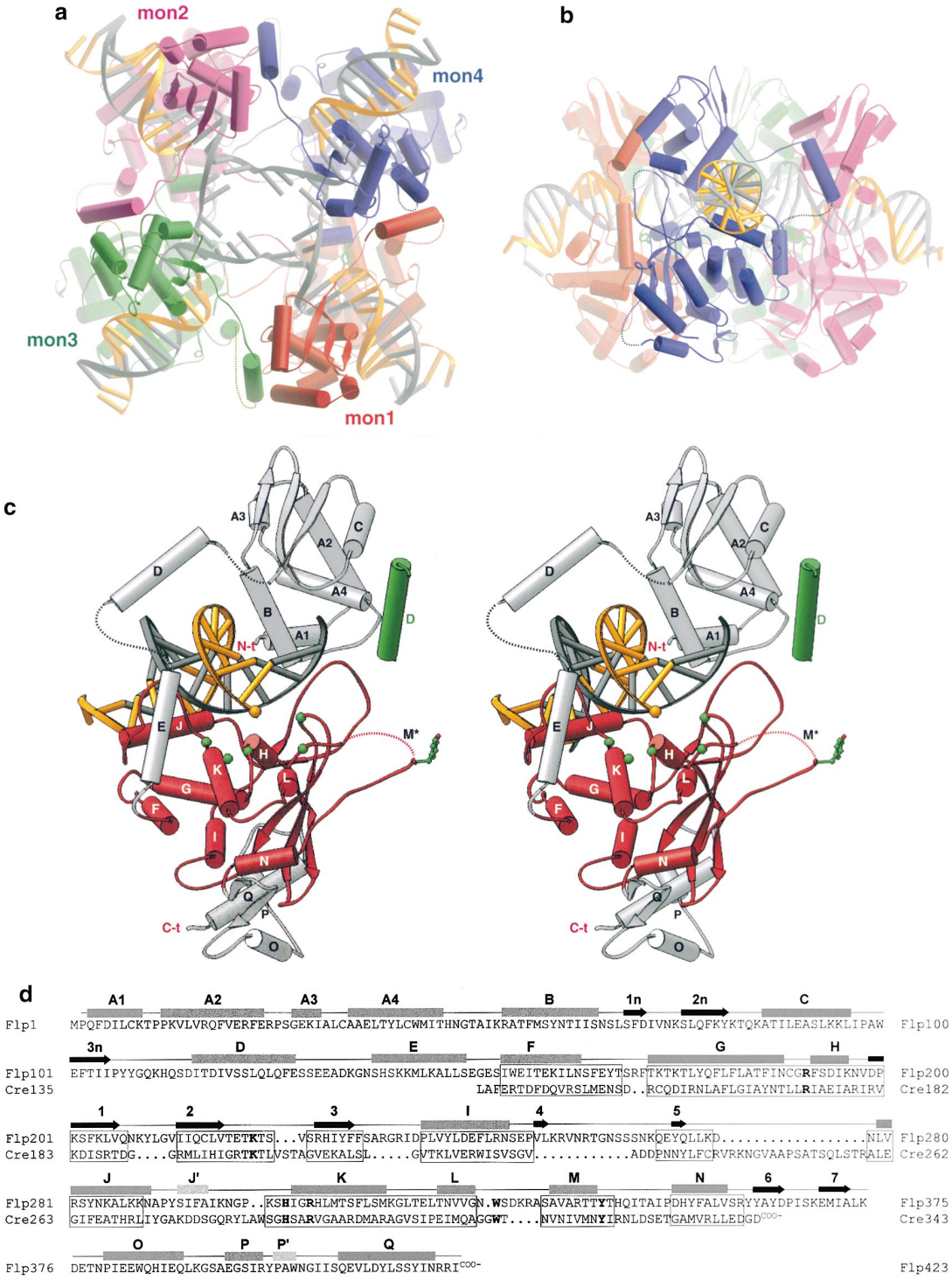

Figure 3. Structure of the Flp–DNA Complex

(a) Top view with the N-terminal domain of the protein above the DNA. The top strand of the half-FRT site (Figure 2) is gold, and the bottom is gray. The *trans*-donated active site tyrosine is shown in green. The tyrosine donated by monomer 2 is disordered. Dotted lines represent connections not visible in the electron density.

(b) Side view looking down the DNA segment bound by monomer 4, with the N-terminal domains at the top.

(c) Stereo view of monomer 1. The scissile phosphate is shown as a gold sphere and the Cα's of the catalytic residues R191, K223, H305, R308, and W330 as green spheres. Y343 is also shown. Helix M (asterisk) is disordered in monomers 1 and 2. The portion of Flp that is structurally homologous with Cre is in red, and the Flp secondary structure elements have been named to correlate with Cre's. Helix D from monomer 3 is shown in green.

(d) Secondary structure of Flp recombinase, aligned with Cre in the C-terminal domain.

Amino acids that are important for catalysis are shown in bold. Boxed regions are structurally comparable. J′ and P′ are short 3_{10} helices.

the active site Y343. Within the complex, the monomer forms a ring that fully encircles the bound DNA.

The active site and part of the DNA-binding site reside in the C-terminal domain. Most of this domain, except for the connectivity of helix M, is structurally homologous to the catalytic domains of the other tyrosine recombinases as well as the type IB topoisomerases (Wigley, 1998). Residues 362–423, which comprise a C-terminal extension not found in these structures, do not form an independently folded domain. Instead, they form a β hairpin and three short helices that pack onto the opposite face of the C-terminal domain from the DNA. The hairpin makes some protein–protein contacts within the tetramer, but the main function of this region may be to anchor the returning polypeptide chain after the domain-swapped helix M.

The N-terminal domain, residues 2–107, is structurally unrelated to the N-terminal domains of other family members, and we found no significant structural homologs for it in the protein data bank using the Dali webserver (Holm and Sander, 1993). In agreement with footprinting and cross-linking studies, the N-terminal domain binds the inner portion of the Flp-binding site, on the opposite face of the DNA from the scissile phosphate (Panigrahi and Sadowski, 1994). It interacts with two other regions of the protein: contacts with the C-terminal domain close the monomer into a circle around the DNA, and contacts with helix D of a neighboring monomer stabilize the tetramer.

The connecting region, residues 108–136, consists of a single amphipathic helix (D) flanked by short flexible regions. This helix nestles into a hydrophobic pocket on the N-terminal domain of an adjacent monomer. This *trans* packing may allow stable yet flexible contacts among monomers in the tetramer.

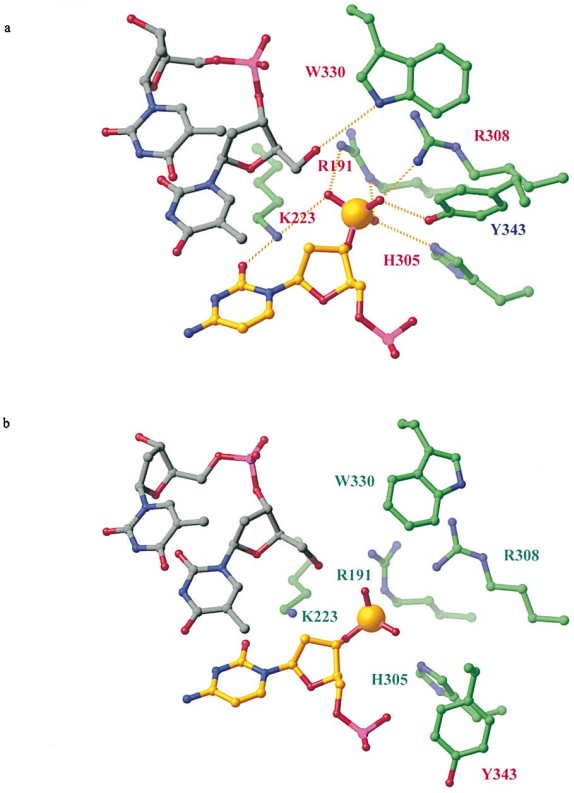

Figure 4. The Two States of the Active Site

(a) The active site residing in monomer 1 (red labels), with the nucleophilic tyrosine provided by monomer 4 (blue label) hydrogen bonded to the scissile phosphate (gold sphere).

(b) The inactive catalytic site of monomer 3 (green labels), with Y343 donated by monomer 1 (red label). This region is less well ordered, thus explicit hydrogen bonds are not shown.

The Active Site Is Assembled in *trans*

A structural feature that distinguishes Flp from other tyrosine recombinases is its helix M, which carries the nucleophile Y343. This helix packs into an adjacent monomer, with its Y343 near the other active site residues from that monomer and the scissile phosphate of the DNA site bound by that protein. Thus, the active site of Flp is assembled in *trans* by domain swapping, as predicted by Jayaram and colleagues (Lee et al., 1999, and references therein). Except for this difference in topology, the active site closely resembles that of Cre and other related enzymes.

As expected from the half-of-the-sites activity of Flp, two conformations of the active site are seen in our complex (Figure 4). These differ most in the positioning of Y343. For the active sites formed within monomers 1 and 2, helix M (donated in *trans* by monomers 4 and 3, respectively) is well ordered, and Y343 is poised to attack the scissile phosphate. In the other pair of active sites, helix M is largely disordered, and although Y343 from monomer 1 can be located in the electron density, its hydroxyl lies almost 10 Å away from its target phosphorus atom. We therefore refer to monomers 1 and 2 as the "active" pair, and monomers 3 and 4 as the "inactive" pair.

Of the other conserved active site residues, R191, H305, and R308 bind the scissile phosphate in both pairs of monomers (Figures 4 and 5). K223 is hydrogen bonded to O2 of the adjacent base, C-5. In the active pair of monomers, it also contacts the scissile phosphate, whereas in the inactive pair, it is less well ordered, and its tip lies closer to the free 5′ hydroxyl than the phosphate. The equivalent lysines in human topoisomerase I and the Cre covalent intermediate form similar hydrogen bonds in the minor groove (Guo et al., 1997; Redinbo et al., 1998). Unlike the small difference seen in Flp, in the inactive Cre monomers this lysine is pulled far away from the active site. In Flp, the position of W330 varies more: in the active pair, it interacts with the free 5′ hydroxyl, but it is farther from the DNA and less well ordered in the inactive pair. Due to hydrolysis of the intermediate, our active site contains one more oxygen atom than it normally would, which may affect the positioning of the surrounding residues.

DNA Structure and Protein–DNA Contacts

The DNA in our crystals is shown in Figure 2. Flp specifically recognizes the 13 bp inverted repeats outside the cleavage points but interacts only nonspecifically with the spacer region. As discussed above, the DNA in the crystal forms a nicked Holliday junction with a seven base spacer. The first three bases of the overhanging bottom strand are base paired with their recombinant partners, although the geometry of the centermost base

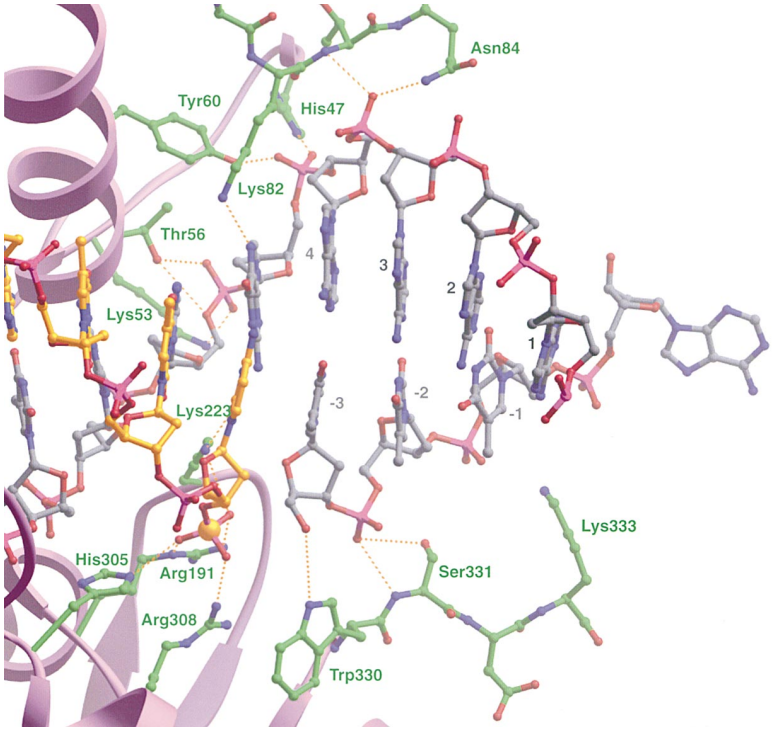

Figure 5. Protein–DNA Contacts in the Spacer Region and Cleavage Site

Monomer 2 is shown, in the same color scheme as Figure 3. The C atoms of protein side chains, DNA top strand, and bottom strand are colored in green, gold, and gray, respectively, and the large gold sphere denotes the scissile phosphate. Hydrogen bonds are shown in dotted lines. Y343 from monomer 3 is also hydrogen bonded to the scissile phosphate but was removed for clarity. These contacts may ensure that the positioning of the 5′ OH of T −3 in the active site is dependent on the formation of Watson-Crick base pairs in the adjacent spacer.

pairs is strained. The central A (#1) is not paired and would form an A:A mismatch if it were. Instead, it stacks on the run of As to its 3′ side.

Within the spacer region, Flp contacts only the outermost two phosphates of each strand, in agreement with solution data (Figure 5) (Bruckner and Cox, 1986). These contacts may ensure that the 5′ hydroxyl is properly positioned for ligation only if the incoming strand can form Watson-Crick base pairs.

Within the Flp recognition site, the protein–DNA interface is similar for all four subunits, and the DNA is essentially B form, with minor variations. Although a single monomer has been reported to induce a 60° bend in the DNA (Schwartz and Sadowski, 1990), we observe only a 24° bend within the recognition site. This discrepancy implies that there may be additional bending in the spacer region or near the scissile phosphate, even when only a monomer is bound.

Most of the contacts seen between Flp and the DNA involve the phosphate backbone rather than the bases. However, there may be additional water-mediated interactions that cannot be detected at the resolution of our structure. Higher resolution structures of Cre show a rather heavily hydrated protein–DNA interface with similarly sparse direct contacts (Guo et al., 1999).

The C-terminal domain, which is largely responsible for the sequence specificity of Flp, spans the major groove at the center of the recognition sequence and contacts both flanking minor grooves as well. Helix J lies in the major groove, and the 24° bend compresses this groove around it. Two residues from this helix contact bases directly: K285 to O2 of T −13, and R281 to O6 and N7 of G11. The importance of this last interaction in specificity is supported by two observations: changes at position 11 result in dramatic defects in recombination (Senecoff et al., 1988), and although several other yeast plasmid recombinases share extensive sequence similarities with Flp, neither R281 nor G11 in their binding sites is conserved (Blaisonneau et al., 1997). The adjacent minor groove, at bp 6–8, is unusually narrow. As the recognition sequence is 5′ ATT here, and A/T-rich sequences correlate with a narrowing of the minor groove (Shatzky-Schwartz et al., 1997), the protein may be using groove width as an indirect determinant of DNA sequence here.

Removal of the outer two base pairs of the recognition site (16 and 17) has little effect on Flp-mediated recombination (Gronostajski and Sadowski, 1985; Jayaram, 1985; Senecoff et al., 1985, 1988). R170 contacts A-16 in the minor groove, which may lend some preference for A:T over G:C base pairs at this position. Base pair 17 is unpaired and poorly ordered in this structure.

The N-terminal domain of Flp binds DNA nonspecifically (Pan and Sadowski, 1993). Only one potentially sequence-specific interaction with this domain is seen: K82 is hydrogen bonded to G5 in the major groove. Helix B lies in the major groove but makes only water-mediated contacts with the bases. Y60, whose mutation causes decreased DNA binding and catalysis (Chen et al., 1991), extends from helix B to contact the phosphate between bases 3 and 4, opposite the scissile phosphate (Figure 5). The N-termini of helices B and A1 also contact phosphates. Interestingly, P2 at the very N terminus of the protein appears to impede the latter interaction, and the mutation P2S significantly improves the thermostability of the reaction (Buchholz et al., 1998).

Isomerization of the Intermediate and Branch Migration

To switch from Holliday junction forming to resolving mode, the complex must isomerize such that the active pair of monomers becomes inactive and vice versa. We

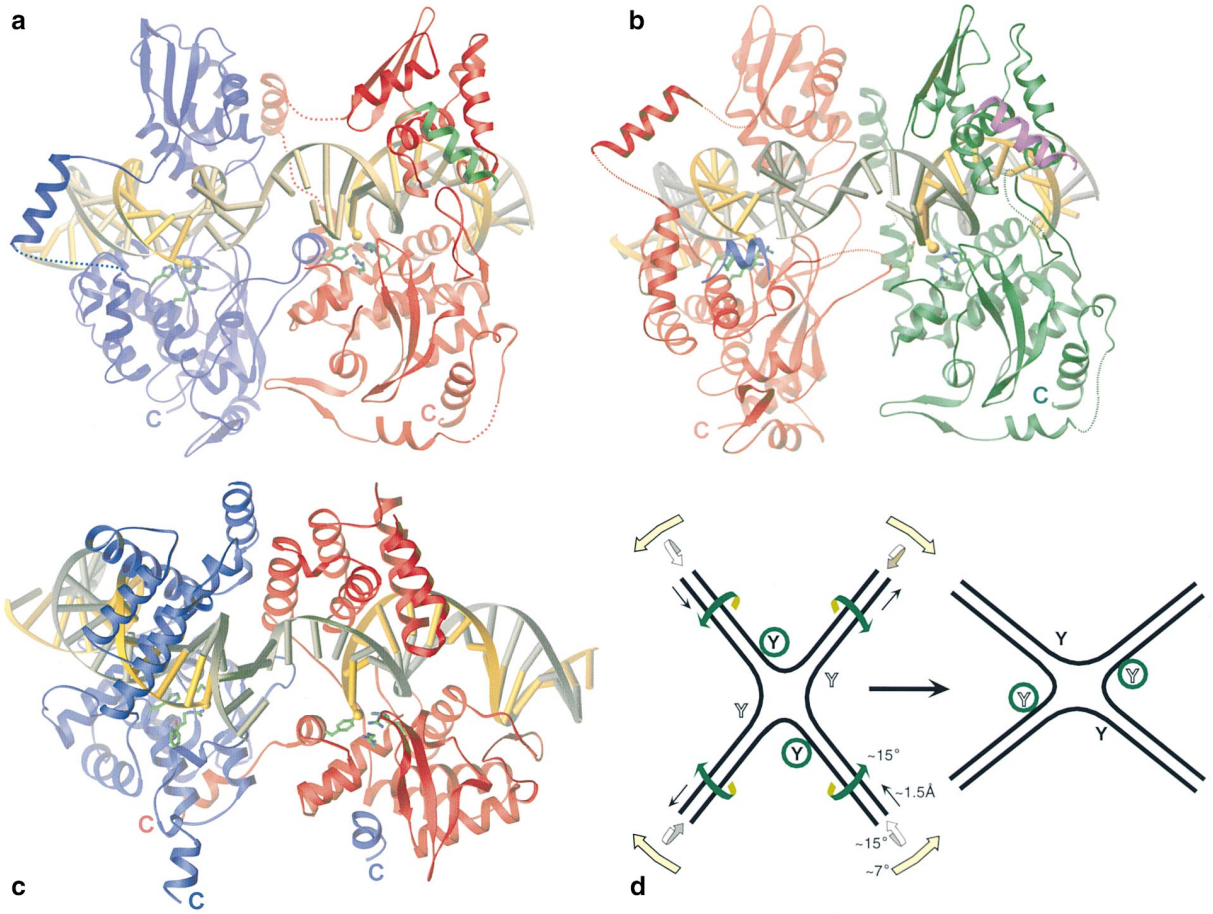

Figure 6. Protein–Protein Interfaces within the Tetramer

(a) Monomers 4 (blue) and 1 (red), viewed from the center of the Holliday junction. This pairing creates a functional active site in monomer 1. Y343, R191, R305, and R308 are shown in green, and the scissile phosphate as gold sphere. Additional *trans* interactions are shown using the same color scheme as Figure 3.

(b) Monomers 1 (red) and 3 (green). Monomer 3 is in the same orientation as monomer 1 in (a). Y343 of monomer 1 can be seen in monomer 3's active site, but it is not properly positioned for catalysis. The C-terminal domains are farther apart in this pairing.

(c) Adjacent monomers in the Cre tetramer (Guo et al., 1997). The active monomer, covalently attached to the scissile phosphate, is in red, and the inactive is in blue. The red monomer's catalytic domain is orientated similarly to monomer 1's in (a). Note the resulting difference in the orientation of the blue catalytic domains. Helix N of the dyad-related blue monomer, which packs into the red one, is also shown.

(d) Proposed Holliday-junction isomerization step for Flp-mediated recombination. Y's represent the nucleophilic tyrosines and the circles show which two are active. The two half-FRT sites under the attack of Y343 are below the plane of the paper, as also shown in Figure 3b. The conformational changes that must occur can be deconvoluted into a translation of each monomer by ~1.5 Å along the DNA axis, followed by three rotations pivoting about the scissile phosphate: a scissoring of the DNA arms by ~7°, then a rotation of ~15° that moves the DNA arms into or below the plane of the junction, followed by a rotation of ~15° around the DNA axis itself.

can model the conformational changes that occur, although not the pathway from one state to the other, by superimposing the two pairs of monomers on one another. This shows that the scissile phosphates move only ~1.5 Å, and the individual monomers swivel about their respective active sites. This isomerization can be described as a small scissoring of the DNA arms, then a rotation that moves the DNA arms of the active monomers ~15° below the plane of the junction, followed by a rotation of ~15° around the DNA axis itself (Figure 6).

This last rotation, coupled with the translation, corresponds to the motions expected for migration of a Holliday junction branch point by about half a base pair. It has been suggested that Flp-mediated recombination would entail limited branch migration. Cre, with a 6 bp spacer, exchanges strands by simply swapping three bases, isomerizing, then swapping the other three, as drawn in Figure 1. For systems with 7 or 8 bp spacers, such as Flp, it was suggested that outer bases would be exchanged by the same mechanism, but the central one or two would be exchanged by migration of the junction branch point (Lee and Jayaram, 1995; Voziyanov et al., 1999). However, not only is the magnitude of the branch migration derived from the Flp structure much smaller than this proposal predicts (15° rotation versus 35° or 70°), but also the direction is opposite to that predicted. It would stabilize base pairing toward the end of the spacer where cleavage can occur and destabilize base pairing on the side of the inactive catalytic site.

Rather than aiding in strand exchange directly, this pseudo-branch migration may help to stabilize the nicked Holliday junction that is perhaps the least stable reaction intermediate. In order to catalyze recombination, Flp must stabilize not only the transition state of the phospho-transfer reactions, but also the topological intermediates of the strand exchange process. Although the protein–protein contacts in the synaptic complex clearly aid in this, the complex must be able to dissociate or the enzyme would not turn over (Waite and Cox, 1995). The intermediate in which the strands have been exchanged but not yet religated to form a covalent Holliday junction may therefore require extra stabilization. Stabilizing the newly formed base pairs in the vicinity of the nick may aid in this.

The isomerization process necessitates changes in monomer–monomer interactions that may explain the regulation of the catalytic activity. The interface between monomers 4 and 1, which cooperate to form a functional active site, is tighter than that between monomers 1 and 3, which form an inactive catalytic center (Figure 6a versus Figure 6b). The rotation of the individual monomers about the DNA helix axis twists the C-terminal domains closer together in the former case. These rotations break the four-fold symmetry of the complex and render it impossible for a particular monomer to form identical protein–protein interfaces with both neighbors. This in itself may enforce the half-of-the-sites activity of the enzyme.

At a more detailed level, isomerization readjusts the segments flanking the domain-swapped helix M that may play a key role in positioning Y343 in the active site. In all four monomers, the C terminus of the helix M-N turn is anchored to its original monomer by the packing of I347 and I350. In monomers 3 and 4, whose Y343 is properly positioned for catalysis, H345 fits into a pocket on the neighboring monomer, between helix E and H309. This places the side chain of H345 over the C terminus of helix M, which it could stabilize by interacting with the helix dipole. As the same segment from monomers 1 and 2 must traverse a greater distance, H345 cannot reach into the neighboring monomer. Instead, T344 occupies roughly the same pocket, but with different phi/psi angles. The importance of H345 in orienting Y343 was suggested by the observation that an H345L mutant of Flp could not catalyze the cleavage step of recombination but was as active as WT Flp in religating substrates already containing a 3′ phosphotyrosine (Kulpa et al., 1993; Pan et al., 1993). The segment between helices L and M must also traverse a longer distance in monomers 1 and 2 than in monomers 3 and 4. This loop and helix M are disordered in monomers 1 and 2, and model building suggests that helix M of these monomers may need to unravel in order for the polypeptide chain to reach from the C terminus of helix L to Y343 in the active site of the neighboring monomer. These observations imply that regardless of the length of the spacer DNA, the dimeric arrangement that forms an active catalytic center remains constant. However, there are probably other more subtle factors involved in determining which pair of catalytic centers is active that cannot all be determined from one structure.

As discussed below, the turn between helices M and N crosses between monomers in the Cre complex as well. This turn may be important in regulating catalysis in Cre as well, but the details of the contacts that it makes are quite different, as the relative orientation of the two monomers it connects is different. H345 is fairly well conserved among tyrosine recombinases, but helix E that forms part of the pocket that it packs into does not exist in Cre, and the equivalent R326 in Cre makes different interactions.

Comparison of Flp and Cre Synaptic Complexes

With the exception of helix E, some loops, and the C-terminal extension of Flp, the catalytic domains of Cre and Flp can be superimposed with an rms distance of 2.5 Å (146 paired Cα's, including domain-swapped helices from neighboring monomers). Flp and Cre also share a common reaction mechanism, including half-of-the-sites activity, and a similar geometry for the DNA strand exchange. Outside of the catalytic domains, however, there is only superficial similarity in their tertiary structures (Figure 6c). The protein–protein interactions, therefore, provide an interesting point of contrast.

Both recombinases must be capable of reversible oligomerization in order to turn over. They use the same helix-swapping strategy to stabilize the oligomer but choose different helices to swap. In Cre, helix N packs onto a neighboring monomer, whereas in Flp helix M, carrying the catalytic tyrosine, is swapped to the neighbor. The turn between helices M and N crosses between monomers in both enzymes; however, in the Flp case, it returns the polypeptide chain back to the original monomer (Figure 6b). This arrangement closely resembles that suggested by Gopaul and Van Duyne (1999).

The Flp and Cre synaptic complexes are both pseudo-four-fold symmetric, but the relative orientation of the individual catalytic domains within the complexes differs. Relative to Cre, each Flp monomer is farther from the center of the Holliday junction and rotated about the axis of the DNA duplex to which it is bound. This correlates with the longer spacer in the Flp structure (seven bases versus six for Cre). It changes the relative orientations of the monomers, such that even without the differences in helix swapping, the protein–protein contacts would vary. In both systems, the N-terminal domains also make important protein–protein contacts, which necessarily differ as these domains are structurally unrelated.

In general, the Flp synaptic complex appears more flexible than that of Cre. The N-terminal domains of Cre pack directly against one another, rather than being linked through flexible loops as in Flp. Isomerization of the Holliday junction intermediate in the Cre case entails only a small scissoring of the DNA arms and the C-terminal domains, with almost no motion of the N-terminal domains, as opposed to the larger and more complicated rotations described above for Flp. This additional flexibility may explain Flp's ability to catalyze recombination of DNA sites with variable spacer lengths.

Relationship with Topoisomerases

The catalytic domain structure that is conserved between Flp and other site-specific recombinases is remarkably similar to that of the type IB topoisomerases (reviewed in Wigley, 1998). These enzymes also share

a common reaction mechanism involving a 3′ phosphotyrosine intermediate, and a nearly identical constellation of active site amino acids. Our structure thus provides further support for an evolutionary relationship between these two families of enzymes.

Another feature shared among the recombinases and type IB topoisomerases is their bipartite clamp shape, in which the catalytic and N-terminal domains bind to opposite faces of the DNA. However, the structural conservation seen in the catalytic domains does not extend to the N-terminal domains. In fact, some tyrosine recombinases function with no N-terminal domain (Nunes-Duby et al., 1998). This implies that the catalytic domains of these enzymes share a common ancestor but that the N-terminal domains have been added in a modular fashion. Given that the only structural similarity between Flp and Cre is in this catalytic domain, it is possible that they diverged separately from ancestral topoisomerases, rather than sharing a common recombinase ancestor. The pseudo-four-fold symmetry of their synaptic complexes may have evolved convergently because the strand exchange reaction is simplest when the Holliday junction is held in a square planar conformation.

Catalysis and Oligomerization: Why *trans*?

It has been suggested that DNA relaxing, or "topoisomerase", activity may result from separating DNA cleavage and religation from synapsis (Wigley, 1998). Prior experiments have demonstrated that Cre can act as a topoisomerase under specific conditions where synaptic complex is unable to assemble (Abremski et al., 1986). Other studies lend support to this hypothesis by showing that vaccinia topoisomerase could resolve certain Holliday junctions (Sekiguchi et al., 1996).

The biological significance of further uncoupling the phosphodiester activation and attacking abilities in Flp, which is the basis for the *trans* cleavage mechanism, is less clear. It does prevent Flp from functioning as a topoisomerase by making cleavage dependent upon dimerization. Flp only displays topoisomerase activity in the presence of an excess of an exogenous nucleophile such as tyramine (Xu et al., 1998). However, the biological pressure against such activity is unclear. The *trans* mechanism also may make the half-of-the-sites activity easier to enforce, thus reducing the probability of accidentally introducing a double-strand break (Lee and Jayaram, 1993).

The *trans* architecture may also endow Flp with an additional "safety" feature germane to its role in 2 μm plasmid replication and analogous to the role of a recently discovered yeast Tyr-DNA phosphodiesterase (Yang et al., 1996; Pouliot et al., 1999). Topoisomerase IB reactions occasionally fail at the religation step. This phosphodiesterase helps repair the resulting DNA lesion by hydroylzing the phosphotyrosine bond that links the defunct topoisomerase to the 3′ end of the DNA. Such dead-end complexes could also be a problem for the 2 μm plasmid recombination process catalyzed by Flp (Sadowski, 1995), as these reactions usually happen during DNA replication and collision with a passing replication fork could lead to the premature disruption of Flp synaptic complexes. In this case, another Flp monomer, instead of a special enzyme, may be sufficient to resolve the covalent linkage between the tyrosine and DNA, even if the original attacking Flp monomer has become denatured and/or degraded. In vitro experiments have shown that Flp can catalyze ligation of DNA substrates that contain Flp-binding sites and 3′-phosphates previously activated by attaching tyrosine residues to them (Pan and Sadowski, 1992). The *trans* architecture thus allows the active site that activates the phosphodiester bond to accept an exogenous tyrosine leaving group/nucleophile. This may enable Flp to function as both Tyr-DNA phosphodiesterase and ligase under such circumstances in vivo.

The use of *trans* cleavage in catalysis is also observed in Flp homologs from other yeast strains (Yang and Jayaram, 1994). Recent structural and biochemical studies indicate that two homodimeric type II topoisomerases, *E. coli* gyrase and yeast topoisomerase II, also have such an intermolecular active site (Morais Cabral et al., 1997; Liu and Wang, 1998). So far, however, the tyrosine recombinases comprise the only family where both *cis* and *trans* cleaving members can be found.

Experimental Procedures

Complex Preparation and Crystallization

Flp protein was purified as described by Sadowski and colleagues (Pan et al., 1991) with several modifications. Primarily, an FRT-DNA affinity column was inserted before the final mono S column (Biorad). The affinity column was prepared according to a published procedure (Meyer-Leon et al., 1987), with oligonucleotides synthesized by the University of Wisconsin Biochemistry Department Synthesis Facility and Operon Technologies. Other purification steps included a Biorex-70 cation exchange column, ammonium sulfate precipitation, and an S-300 gel filtration column. All purification procedures were carried out at 4°C.

Synthetic oligonucleotides for complex preparation were purchased from the Keck biotechnology facility at Yale University with the 5′-trityl on. They were purified by reverse phase HPLC on a C4 column (in 25 mM ammounium acetate [pH 6.0], eluting with an acetonitrile gradient), followed by mild acetic acid treatment to remove the trityl group, and rechromatographing on the same column.

To prepare the Flp–DNA complex, Flp protein (0.34 mM, in 0.75 M NaCl) and annealed DNA duplex (1 mM) were mixed at a 1:3 molar ratio and dialyzed against buffer containing 0.1 M NaCl, 10 mM HEPES (pH 7.0), and 2 mM dithiothreitol (DTT). This was based on the observation that Flp protein is only soluble at high salt, whereas the DNA complex is soluble in 0.1 M NaCl (lype, 1995). A variety of DNA substrates with different end configurations and spacer sequences were tested for crystallization. The best crystals were obtained with the substrate shown in Figure 2b.

Crystals were grown at 4°C using the hanging drop method. In the initial drops, 1.5 μl complex solution prepared as described above was mixed with 3 μl reservoir containing 0.1 M NaCl, 20 mM HEPES (pH 7.0), 10 mM $CaCl_2$, 20% glycerol, 2 mM DTT, and 12% polyethylene glycol 5000 monomethyl ether. Crystals appeared after 3–7 days and reached a maximal size of 0.2 × 0.2 × 0.4 mm in 3–4 weeks. They are in space group $P2_1$, with unit cell dimensions of 80 Å, 180 Å, 97 Å, 90°, 95.7°, 90°, and contain a DNA-bound tetramer in the asymmetric unit. Bromine derivatives were obtained using modified oligonucleotides with their thymine bases replaced by 5-bromo-uracils. Two modified versions of the top strand (Figure 2b) were used: T_{br3}, TAAGUTCCUATUCT, had three bromo-uracils ("U"), while T_{br4}, UAAGUUCCUAUUCU, had all thymines substituted. Mercury derivatives, "Mercury1" and "Mercury2" in Table 1, were prepared by soaking crystals in solutions of mercury acetate (0.15 mM) and thimerosyl (8 mM) for 24 hr, respectively. The "Mercury3" data were collected from a derivative obtained by adding 30 μl 0.15 mM mercury acetate solution directly to the drop and flash-freezing 24 hr later.

Structure Determination and Refinement

Crystals were mounted on nylon loops (Hampton Research) and flash-frozen in liquid propane before data collection at 100–110K. Data were collected on an R-Axis IIc image-plate detector mounted on a Rigaku RU200 rotating anode equipped with focusing mirrors (MSC) and at the BioCARS 14BM-D beamline at the Advanced Photon Source using an ADSC 1K CCD detector. Raw data were reduced and scaled with the HKL suite (Otwinowski and Minor, 1997). Hg sites were initially found by SOLVE (Terwilliger and Berendzen, 1999) combined with visual inspection of Patterson maps. The positions of the Br atoms in the MAD data were determined by anomalous difference Fourier, using phases calculated from the Hg positions. MLPHARE was used for refinement of heavy-atom positions and phase calculations, with the MAD data treated as a special case of MIR (Otwinowski, 1993). Initial phases were calculated to 3.10 Å resolution and improved and extended to 2.65 Å by solvent flattening, histogram matching, and four-fold averaging, using the DM program of the CCP4 suite and a mask created by MAMA (Bailey, 1994; Kleywegt and Jones, 1994; Cowtan and Zhang, 1999). The model was built into the experimental density maps using the program O (Jones et al., 1991).

Refinement was done by the program CNS_SOLVE, using simulated annealing and energy minimization (Brunger et al., 1998). The protein parameters of Engh and Huber and the DNA parameters of Berman and colleagues were used (Engh and Huber, 1991; Parkinson et al., 1996). During the initial refinement, the phases were restrained to those of the experimental electron density map, and strong four-fold noncrystallographic symmetry (NCS) restraints were applied. As refinement progressed, conformational differences between pairs of monomers became apparent. Two-fold NCS restraints were then used, with pairs of N- and C-terminal domains restrained separately. All residues involved in crystal packing were also removed from the NCS restraints. Phases from the refined model were combined with experimental phases to generate improved electron density maps, which were used in subsequent model rebuilding.

The DNA structure was analyzed with CURVES (Lavery and Sklenar, 1989), and all figures showing the structure were prepared using RIBBONS (Carson, 1997).

Acknowledgments

We thank Kerren Swinger, Carl Correll, and the staff of BioCARS for help with synchrotron data collection. This research was supported by National Institutes of Health grant GM58827 (to P. A. R.).

Received June 15, 2000; revised August 11, 2000.

References

Abremski, K.E., and Hoess, R.H. (1992). Evidence for a second conserved arginine residue in the integrase family of recombination proteins. Protein Eng. *5*, 87–91.

Abremski, K., Wierzbicki, A., Frommer, B., and Hoess, R.H. (1986). Bacteriophage P1 Cre-loxP site-specific recombination. Site-specific DNA topoisomerase activity of the Cre recombination protein. J. Biol. Chem. *261*, 391–396.

Arciszewska, L.K., and Sherratt, D.J. (1995). Xer site-specific recombination in vitro. EMBO J. *14*, 2112–2120.

Argos, P., Landy, A., Abremski, K., Egan, J.B., Haggard-Ljungquist, E., Hoess, R.H., Kahn, M.L., Kalionis, B., Narayana, S.V., Pierson, L.S.D., et al. (1986). The integrase family of site-specific recombinases: regional similarities and global diversity. EMBO J. *5*, 433–440.

Bailey, S. (1994). The Ccp4 suite: programs for protein crystallography. Acta Crystallogr. D *50*, 760–763.

Blaisonneau, J., Sor, F., Cheret, G., Yarrow, D., and Fukuhara, H. (1997). A circular plasmid from the yeast *Torulaspora delbrueckii*. Plasmid *38*, 202–209.

Blakely, G.W., Davidson, A.O., and Sherratt, D.J. (1997). Binding and cleavage of nicked substrates by site-specific recombinases XerC and XerD. J. Mol. Biol. *265*, 30–39.

Bruckner, R.C., and Cox, M.M. (1986). Specific contacts between the FLP protein of the yeast 2-micron plasmid and its recombination site. J. Biol. Chem. *261*, 11798–11807.

Brunger, A.T., Adams, P.D., Clore, G.M., DeLano, W.L., Gros, P., Grosse-Kunstleve, R.W., Jiang, J.S., Kuszewski, J., Nilges, M., Pannu, N.S., et al. (1998). Crystallography & NMR system: a new software suite for macromolecular structure determination. Acta Crystallogr. D *54*, 905–921.

Buchholz, F., Angrand, P.O., and Stewart, A.F. (1998). Improved properties of FLP recombinase evolved by cycling mutagenesis. Nat. Biotechnol. *16*, 657–662.

Carson, M. (1997). RIBBONS. Macromol. Crystallogr. Pt B *277*, 493–505.

Chen, J.W., Evans, B.R., Zheng, L., and Jayaram, M. (1991). Tyr60 variants of Flp recombinase generate conformationally altered protein-DNA complexes. Differential activity in full-site and half-site recombinations. J. Mol. Biol. *218*, 107–118.

Chen, J.W., Evans, B.R., Yang, S.H., Araki, H., Oshima, Y., and Jayaram, M. (1992). Functional analysis of box I mutations in yeast site-specific recombinases Flp and R: pairwise complementation with recombinase variants lacking the active-site tyrosine. Mol. Cell Biol. *12*, 3757–3765.

Cheng, C., Kussie, P., Pavletich, N., and Shuman, S. (1998). Conservation of structure and mechanism between eukaryotic topoisomerase I and site-specific recombinases. Cell *92*, 841–850.

Cowtan, K.D., and Zhang, K.Y.J. (1999). Density modification for macromolecular phase improvement. Prog. Biophys. Molec. Biol. *72*, 245–270.

Crisona, N.J., Weinberg, R.L., Peter, B.J., Sumners, D.W., and Cozzarelli, N.R. (1999). The topological mechanism of phage lambda integrase. J. Mol. Biol. *289*, 747–775.

Engh, R.A., and Huber, R. (1991). Accurate bond and angle parameters for X-ray protein-structure refinement. Acta Crystallogr. A *47*, 392–400.

Esposito, D., and Scocca, J.J. (1997). The integrase family of tyrosine recombinases: evolution of a conserved active site domain. Nucleic Acids Res. *25*, 3605–3614.

Gillette, W.K., Rhee, S., Rosner, J.L., and Martin, R.G. (2000). Structural homology between MarA of the AraC family of transcriptional activators and the integrase family of site-specific recombinases. Mol. Microbiol. *35*, 1582–1583.

Gopaul, D.N., and Van Duyne, G.D. (1999). Structure and mechanism in site-specific recombination. Curr. Opin. Struct. Biol. *9*, 14–20.

Gopaul, D.N., Guo, F., and Van Duyne, G.D. (1998). Structure of the Holliday junction intermediate in Cre-loxP site- specific recombination. EMBO J. *17*, 4175–4187.

Grainge, I., and Jayaram, M. (1999). The integrase family of recombinase: organization and function of the active site. Mol. Microbiol. *33*, 449–456.

Gronostajski, R.M., and Sadowski, P.D. (1985). Determination of DNA sequences essential for FLP-mediated recombination by a novel method. J. Biol. Chem. *260*, 12320–12327.

Guo, F., Gopaul, D.N., and Van Duyne, G.D. (1997). Structure of Cre recombinase complexed with DNA in a site-specific recombination synapse. Nature *389*, 40–46.

Guo, F., Gopaul, D.N., and Van Duyne, G.D. (1999). Asymmetric DNA bending in the Cre-loxP site-specific recombination synapse. Proc. Natl. Acad. Sci. USA *96*, 7143–7148.

Hallet, B., Arciszewska, L.K., and Sherratt, D.J. (1999). Reciprocal control of catalysis by the tyrosine recombinases XerC and XerD: an enzymatic switch in site-specific recombination. Mol. Cell *4*, 949–959.

Hickman, A.B., Waninger, S., Scocca, J.J., and Dyda, F. (1997). Molecular organization in site-specific recombination: the catalytic domain of bacteriophage HP1 integrase at 2.7 Å resolution. Cell *89*, 227–237.

Hoess, R.H., Ziese, M., and Sternberg, N. (1982). P1 site-specific recombination: nucleotide sequence of the recombining sites. Proc. Natl. Acad. Sci. USA *79*, 3398–3402.

Holm, L., and Sander, C. (1993). Protein structure comparison by alignment of distance matrices. J. Mol. Biol. *233*, 123–138.

Huffman, K.E., and Levene, S.D. (1999). DNA-sequence asymmetry directs the alignment of recombination sites in the FLP synaptic complex. J. Mol. Biol. *286*, 1–13.

Iype, L.E. (1995). Studies of recombination proteins in homologous and site-specific DNA recombination (*Escherichia coli, Saccharomyces cerevisiae*). Ph.D. dissertation, University of Wisconsin-Madison, Madison, WI.

Jayaram, M. (1985). Two-micrometer circle site-specific recombination: the minimal substrate and the possible role of flanking sequences. Proc. Natl. Acad. Sci. USA *82*, 5875–5879.

Jayaram, M. (1997). The cis-trans paradox of integrase. Science *276*, 49–51.

Jones, T.A., Zou, J.Y., Cowan, S.W., and Kjeldgaard, M. (1991). Improved methods for building protein models in electron-density maps and the location of errors in these models. Acta Crystallogr. A *47*, 110–119.

Kleywegt, G.J., and Jones, T.A. (1994). Halloween . . . masks and bones. In From First Map to Final Model, S. Bailey, R. Hubbard, and D. Waller, eds. (Warrington, England: SERC Daresbury Laboratory), pp. 59–66.

Knudsen, B.R., Dahlstrom, K., Westergaard, O., and Jayaram, M. (1997). The yeast site-specific recombinase Flp mediates alcoholysis and hydrolysis of the strand cleavage product: mimicking the strand-joining reaction with non-DNA nucleophiles. J. Mol. Biol. *266*, 93–107.

Krogh, B.O., and Shuman, S. (2000). Catalytic mechanism of DNA topoisomerase IB. Mol. Cell *5*, 1035–1041.

Kulpa, J., Dixon, J.E., Pan, G., and Sadowski, P.D. (1993). Mutations of the FLP recombinase gene that cause a deficiency in DNA bending and strand cleavage. J. Biol. Chem. *268*, 1101–1108.

Kwon, H.J., Tirumalai, R., Landy, A., and Ellenberger, T. (1997). Flexibility in DNA recombination: structure of the lambda integrase catalytic core. Science *276*, 126–131.

Laskowski, R.A., Macarthur, M.W., Moss, D.S., and Thornton, J.M. (1993). Procheck: a program to check the stereochemical quality of protein structures. J. Appl. Crystallogr. *26*, 283–291.

Lavery, R., and Sklenar, H. (1989). Defining the structure of irregular nucleic-acids-conventions and principles. J. Biomol. Struct. Dynam. *6*, 655–667.

Lee, J., and Jayaram, M. (1993). Mechanism of site-specific recombination. Logic of assembling recombinase catalytic site from fractional active sites. J. Biol. Chem. *268*, 17564–17570.

Lee, J., and Jayaram, M. (1995). Role of partner homology in DNA recombination. Complementary base pairing orients the 5′-hydroxyl for strand joining during Flp site-specific recombination. J. Biol. Chem. *270*, 4042–4052.

Lee, J., Jayaram, M., and Grainge, I. (1999). Wild-type Flp recombinase cleaves DNA in trans. EMBO J. *18*, 784–791.

Liu, Q., and Wang, J.C. (1998). Identification of active site residues in the "GyrA" half of yeast DNA topoisomerase II. J. Biol. Chem. *273*, 20252–20260.

Meyer-Leon, L., Gates, C.A., Attwood, J.M., Wood, E.A., and Cox, M.M. (1987). Purification of the FLP site-specific recombinase by affinity chromatography and re-examination of basic properties of the system. Nucleic Acids Res *15*, 6469–6488.

Morais Cabral, J.H., Jackson, A.P., Smith, C.V., Shikotra, N., Maxwell, A., and Liddington, R.C. (1997). Crystal structure of the breakage-reunion domain of DNA gyrase. Nature *388*, 903–906.

Nagy, A. (2000). Cre recombinase: the universal reagent for genome tailoring. Genesis *26*, 99–109.

Nunes-Duby, S.E., Matsumoto, L., and Landy, A. (1987). Site-specific recombination intermediates trapped with suicide substrates. Cell *50*, 779–788.

Nunes-Duby, S.E., Tirumalai, R.S., Dorgai, L., Yagil, E., Weisberg, R.A., and Landy, A. (1994). Lambda integrase cleaves DNA in cis. EMBO J. *13*, 4421–4430.

Nunes-Duby, S.E., Kwon, H.J., Tirumalai, R.S., Ellenberger, T., and Landy, A. (1998). Similarities and differences among 105 members of the Int family of site-specific recombinases. Nucleic Acids Res. *26*, 391–406.

O'Gorman, S., and Wahl, G.M. (1997). Mouse engineering. Science *277*, 1025.

Otwinowski, Z. (1993). Maximum likelihood refinement of heavy atom parameters. In Isomorphous Replacement and Anomalous Scattering, W. Wolf, P.R. Evans, and A.G.W. Leslie, eds. (Warrington, England: SERC Daresbury Laboratory), pp. 80–86.

Otwinowski, Z., and Minor, W. (1997). Processing of X-ray diffraction data collected in oscillation model. Macromol. Crystallogr. Pt A *276*, 307–326.

Pan, G., and Sadowski, P.D. (1992). Ligation activity of FLP recombinase. The strand ligation activity of a site-specific recombinase using an activated DNA substrate. J. Biol. Chem. *267*, 12397–12399.

Pan, G., and Sadowski, P.D. (1993). Identification of the functional domains of the FLP recombinase. Separation of the nonspecific and specific DNA-binding, cleavage, and ligation domains. J. Biol. Chem. *268*, 22546–22551.

Pan, H., Clary, D., and Sadowski, P.D. (1991). Identification of the DNA-binding domain of the FLP recombinase. J. Biol. Chem. *266*, 11347–11354.

Pan, G., Luetke, K., and Sadowski, P.D. (1993). Mechanism of cleavage and ligation by FLP recombinase: classification of mutations in FLP protein by in vitro complementation analysis. Mol. Cell Biol. *13*, 3167–3175.

Panigrahi, G.B., and Sadowski, P.D. (1994). Interaction of the NH2- and COOH-terminal domains of the FLP recombinase with the FLP recognition target sequence. J. Biol. Chem. *269*, 10940–10945.

Parkinson, G., Vojtechovsky, J., Clowney, L., Brunger, A.T., and Berman, H.M. (1996). New parameters for the refinement of nucleic acid-containing structures. Acta Crystallogr. D *52*, 57–64.

Pouliot, J.J., Yao, K.C., Robertson, C.A., and Nash, H.A. (1999). Yeast gene for a Tyr-DNA phosphodiesterase that repairs topoisomerase I complexes. Science *286*, 552–555.

Qian, X.H., and Cox, M.M. (1995). Asymmetry in active complexes of FLP recombinase. Genes Dev. *9*, 2053–2064.

Redinbo, M.R., Stewart, L., Kuhn, P., Champoux, J.J., and Hol, W.G. (1998). Crystal structures of human topoisomerase I in covalent and noncovalent complexes with DNA. Science *279*, 1504–1513.

Redinbo, M.R., Champoux, J.J., and Hol, W.G. (2000). Novel insights into catalytic mechanism from a crystal structure of human topoisomerase I in complex with DNA. Biochemistry *39*, 6832–6840.

Sadowski, P.D. (1995). The Flp recombinase of the 2-microns plasmid of Saccharomyces cerevisiae. Prog. Nucleic Acid Res. Mol. Biol. *51*, 53–91.

Schwartz, C.J., and Sadowski, P.D. (1990). FLP protein of 2 mu circle plasmid of yeast induces multiple bends in the FLP recognition target site. J. Mol. Biol. *216*, 289–298.

Sekiguchi, J., Seeman, N.C., and Shuman, S. (1996). Resolution of Holliday junctions by eukaryotic DNA topoisomerase I. Proc. Natl. Acad. Sci. USA *93*, 785–789.

Senecoff, J.F., and Cox, M.M. (1986). Directionality in FLP protein-promoted site-specific recombination is mediated by DNA-DNA pairing. J. Biol. Chem. *261*, 7380–7386.

Senecoff, J.F., Bruckner, R.C., and Cox, M.M. (1985). The FLP recombinase of the yeast 2-micron plasmid: characterization of its recombination site. Proc. Natl. Acad. Sci. USA *82*, 7270–7274.

Senecoff, J.F., Rossmeissl, P.J., and Cox, M.M. (1988). DNA recognition by the FLP recombinase of the yeast 2 mu plasmid. A mutational analysis of the FLP binding site. J. Mol. Biol. *201*, 405–421.

Shatzky-Schwartz, M., Arbuckle, N.D., Eisenstein, M., Rabinovich, D., Bareket-Samish, A., Haran, T.E., Luisi, B.F., and Shakked, Z. (1997). X-ray and solution studies of DNA oligomers and implications for the structural basis of A-tract-dependent curvature. J. Mol. Biol. *267*, 595–623.

Sternberg, N., and Hamilton, D. (1981). Bacteriophage P1 site-spe-

cific recombination. I. Recombination between loxP sites. J. Mol. Biol. *150*, 467–486.

Subramanya, H.S., Arciszewska, L.K., Baker, R.A., Bird, L.E., Sherratt, D.J., and Wigley, D.B. (1997). Crystal structure of the site-specific recombinase, XerD. EMBO J. *16*, 5178–5187.

Terwilliger, T.C., and Berendzen, J. (1999). Automated MAD and MIR structure solution. Acta Crystallogr. D *55*, 849–861.

Voziyanov, Y., Pathania, S., and Jayaram, M. (1999). A general model for site-specific recombination by the integrase family recombinases. Nucleic Acids Res. *27*, 930–941.

Waite, L.L., and Cox, M.M. (1995). A protein dissociation step limits turnover in FLP recombinase-mediated site-specific recombination. J. Biol. Chem. *270*, 23409–23414.

Wigley, D.B. (1998). Teaching a new dog old tricks? Structure *6*, 543–548.

Xu, C.J., Grainge, I., Lee, J., Harshey, R.M., and Jayaram, M. (1998). Unveiling two distinct ribonuclease activities and a topoisomerase activity in a site-specific DNA recombinase. Mol.Cell *1*, 729–739.

Yang, S.H., and Jayaram, M. (1994). Generality of the shared active site among yeast family site-specific recombinases. The R site-specific recombinase follows the Flp paradigm. J. Biol. Chem. *269*, 12789–12796.

Yang, S.W., Burgin, A.B., Jr., Huizenga, B.N., Robertson, C.A., Yao, K.C., and Nash, H.A. (1996). A eukaryotic enzyme that can disjoin dead-end covalent complexes between DNA and type I topoisomerases. Proc. Natl. Acad. Sci. USA *93*, 11534–11539.

Protein Data Bank ID Code

Coordinates and diffraction data have been deposited with the ID code 1flo.